Pergamon

0277-5387(94)00448-X

Polyhedron Vol. 14, No. 13–14, pp. 1943–1952, 1995

0277–5387/95 $9.50+0.00

CRYSTAL STRUCTURE AND MÖSSBAUER STUDY OF TRILITHIUM IRON(III) TRIOXALATE PENTAHYDRATE

J. P. DECLERCQ* and J. FENEAU-DUPONT

Laboratoire de chimie physique et de cristallographie, Université Catholique de Louvain, 1 place Louis Pasteur, 1348 Louvain la Neuve, Belgium

and

J. LADRIERE

Laboratoire de chimie inorganique et nucléaire, Université Catholique de Louvain, 2 chemin du cyclotron, 1348 Louvain la Neuve, Belgium

(*Received* 6 *September* 1994; *accepted* 24 *October* 1994)

Abstract—The crystal structure of the complex $Li_3[Fe(C_2O_4)_3] \cdot 5H_2O$ has been determined by X-ray diffraction analysis. The coordination of the iron atom is a distorted octahedron composed of the oxygen atoms of three oxalate ions. Two of the lithium ions are octrahedral and the third one is tetrahedral. Infinite chains appear along the *b*-axis, with alternation of Fe^{3+} and Li^+ cations separated by oxalate anions. In agreement with this, the Mössbauer spectrum consists of an asymmetric and strongly broadened absorption pattern, indicating the presence of both paramagnetic relaxation effects and quadrupolar interaction which result from an Fe^{3+} interionic shortest distance of 6.559 Å and from a non-cubic iron environment, respectively.

In a previous study,[1] the Mössbauer spectra of $Li_4Fe(C_2O_4)_3Cl \cdot 9H_2O$ have been interpreted on the basis of both iron coordination geometry and interionic distances obtained from X-ray diffraction analysis on single crystals (XRD).

In the case of alkali trisoxalatoferrate(III), $M_3Fe(C_2O_4)_3 \cdot xH_2O$, the interpretation of the Mössbauer spectra can be made properly only for the few compounds whose crystallographic structure has been well established, namely potassium[2] and ammonium[3] trisoxalatoferrate(III) trihydrate.

In this paper, the detailed crystallographic structure of lithium trisoxalatoferrate(III) pentahydrate, $Li_3Fe(C_2O_4)_3 \cdot 5H_2O$, is determined by X-ray diffraction analysis and the Mössbauer spectrum of ^{57}Fe in this compound is analysed in connection with the crystallographic data.

EXPERIMENTAL

Synthesis and chemical analysis

The green crystals of the complex, $Li_3Fe(C_2O_4)_3 \cdot 5H_2O$, have been obtained by slow evaporation at 45°C, in the dark, from a saturated aqueous solution of pure tetralithium iron(III) trioxalate chloride nonahydrate, $Li_4Fe(C_2O_4)_3Cl \cdot 9H_2O$, a compound already described in a previous study.[1] The crystals of lithium trisoxalatoferrate(III) pentahydrate show an elongated parallelepiped shape, in contrast to the triangular base prismatic shape of $Li_4Fe(C_2O_4)_3Cl \cdot 9H_2O$ which shows, in addition, a flake-like texture parallel to the triangular plane.

The chemical composition of $Li_3Fe(C_2O_4)_3 \cdot 5H_2O$ was determined by elemental analysis of iron and oxalate, using potentiometric titration with Ce^{4+} and Cr^{2+} solutions as oxidizing and reducing reagents, respectively. The observed relative weights of these components are in good agreement

* Author to whom correspondence should be addressed.

with the theoretical values calculated from the above formula. Found: $C_2O_4^{2-}$, 61.5; Fe, 12.4. Calc.: $C_2O_4^{2-}$, 61.3; Fe, 13.0%.

The water of crystallization and lithium contents were obtained from thermogravimetric analysis (TGA) using a Dupont 2000 thermal analyser, the measurements being performed under pure nitrogen at a heating rate of 20°C min^{-1}. The observed weight loss (21.0%) corresponding to the dehydration step (from 120 to 200°C) is in good agreement with the theoretical value (20.9%) calculated for the loss of five water molecules. Furthermore, the lithium content can be determined from the relative weight of the residue obtained at 650°C, which is essentially composed of a mixture of lithium carbonate and metallic iron ($3/2Li_2CO_3 + Fe$). By comparing the observed value (39%) with the theoretical one (38.7%), calculated for the composition of this residue, the observed lithium content (4.8%) was found to agree with the expected value (4.8%).

From the TGA curve (Fig. 1), it can be seen that, after dehydration at 200°C, the anhydrous lithium trisoxalatoferrate(III), $Ll_3Fe(C_2O_4)_3$, undergoes two consecutive transformations similar to those observed previously for other alkali trisoxalatoferrates(III).[4-6] The first one at 275°C corresponds to the reduction of the anhydrous ferric complex into ferrous oxalate, FeC_2O_4; this transformation is characterized by the loss of one carbon dioxide molecule per iron atom and by the formation of a second phase, anhydrous lithium oxalate, $Li_2C_2O_4$. This result does not agree with a previously reported thermal analysis[7] of the same compound, for which a ferric species was obtained after this decomposition stage, either in air or in nitrogen. It is thought that, in the latter case, the presence of residual oxygen is responsible for the oxidation of ferrous oxalate. The last steps of decomposition correspond to the breakdown of both FeC_2O_4 (weight loss 16.7%) and $Li_2C_2O_4$ (weight loss 13.5%), giving rise to the final residue.

The density of $Li_3Fe(C_2O_4)_3 \cdot 5H_2O$ has been measured at 25°C by the pycnometer method in carbon tetrachloride. The measured value (1.875 g cm^{-3}) corresponds fairly well to the value calculated from the unit cell parameters (1.87 g cm^{-3}).

Crystal structure determination of $Li_3Fe(C_2O_4)_3 \cdot 5H_2O$

The crystal used had the shape of a parallelepiped with dimensions $0.4 \times 0.5 \times 0.6$ mm. The centring of 18 reflections in the range of $24° \leqslant 2\theta \leqslant 35°$ allowed refinement of the lattice parameters. Intensity data were collected at room temperature on a Huber four-circle diffractometer, using graphite monochromatized Mo-K_α radiation ($\lambda = 0.71069$ Å). A standard reflection (3,1,4) was checked every 50 reflections, and showed no significant deviation; 9498 independent reflections were collected with $\sin\theta/\lambda \leqslant 0.90$ $Å^{-1}$, of which 7798 with $I \geqslant 2.5\sigma(I)$ were

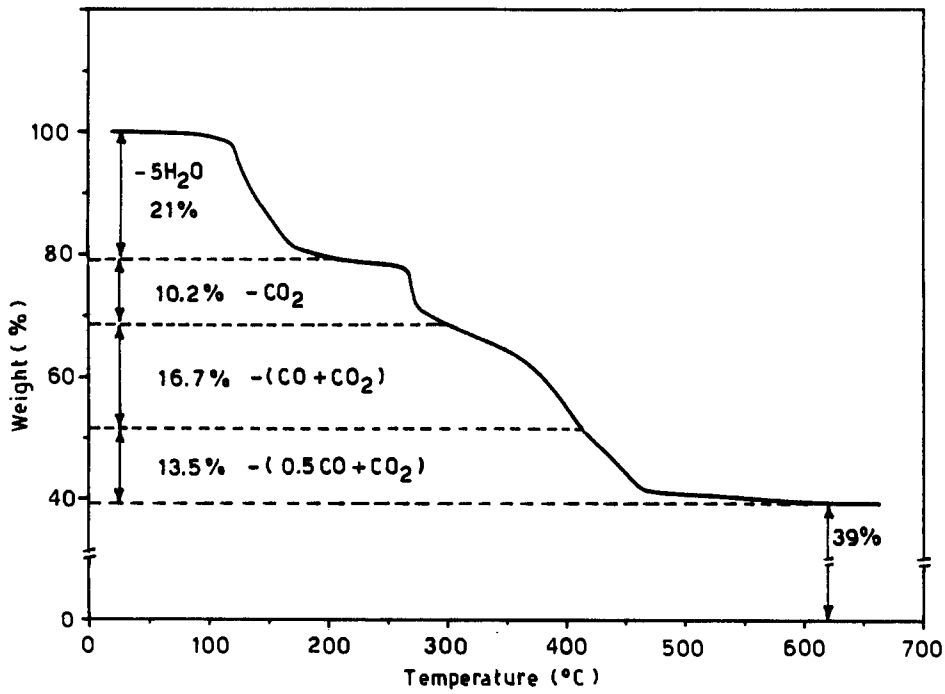

Fig. 1. Thermogravimetric analysis of $Li_3Fe(C_2O_4)_3 \cdot 5H_2O$ in nitrogen.

considered as observed and used in further calculations. An empirical absorption correction based on the collection of Ψ scans was applied to the measured intensities. The crystal data are summarized in Table 1.

The Patterson method as implemented in SHELXS86[8] was used to solve the structure. The positions of the hydrogen atoms of the water molecules were obtained from a difference Fourier synthesis. An anisotropic least squares refinement (SHELX76[9]) using F converged to $R = 0.036$, $R_w = 0.043$ for 7798 observed reflections. For the hydrogen atoms, a common isotropic temperature factor was refined. The atomic scattering factors are from *International Tables for X-ray Crystallography* (1974, Vol. IV). Figure 2 shows one asymmetric unit, with the numbering of the atoms. The bond distances and angles are given in Table 2. Lists of atomic coordinates, anisotropic thermal parameters and observed and calculated structure factors have been deposited as supplementary material with the Editor, from whom copies are available on request.

Mössbauer measurements

The Mössbauer spectra were determined at 298 K, using a constant acceleration spectrometer and a $^{57}Co(Rh)$ source. The measurements have been performed on polycrystalline samples obtained by grinding single crystals in chloroform in order to prevent dehydration. The effective thickness of the absorbers was adjusted to 10 mg cm^{-2} of natural iron. The isomer shift values are reported with respect to α-iron. Experimental data were resolved into Lorentzian lines using an iterative least-square fit program and the goodness of the fit was estimated from the χ^2 values.

Table 1. Crystal data and structure refinement of $Li_3Fe(C_2O_4)_3\cdot 5H_2O$

Formula	$C_6H_{10}O_{17}Li_3Fe$
Formula weight	430.8
Crystal system	triclinic
Space group	$P\bar{1}$
a (Å)	7.892(1)
b (Å)	9.272(1)
c (Å)	11.942(1)
α (°)	104.75(1)
β (°)	101.69(2)
γ (°)	107.92(1)
V (Å^3)	765.7(2)
Z	2
D_c (g cm^{-3})	1.87
D_m (g cm^{-3})	1.875
$F(000)$	434
Wavelength (Å)	0.71069
$(\sin\theta/\lambda)_{max}$ (Å^{-1})	0.90
μ (cm^{-1})	11.1
Data collected	9498
Data with $I \geqslant 2.5\sigma(I)$	7798
Limits of the absorption correction	1.02–1.19
R	0.036
R_w	0.043
S (goodness of fit)	0.87
w	$1/[\sigma^2(F_0)+0.0034F_0^2]$

RESULTS AND DISCUSSION

Description of the structure

Each iron atom is surrounded by six oxygen atoms belonging to the three independent oxalate ions, in a distorted octahedral arrangement. As shown in Fig. 2, these three ions are approximately related by a non-crystallographic three-fold axis through the Fe^{3+} ion. Each oxalate ion acts as a bidentate ligand: two oxygen atoms belonging to two different carboxylate groups are bound to the iron ion, while the two remaining ones are bound to a lithium ion [respectively $Li^+(1)$, $Li^+(2)$ and $Li^+(1)$ translated by one unit-cell in the b-direction]. As shown in Table 2, the six oxygen–iron distances are very similar. Their mean value (2.015 Å) is in good agreement with the mean distances observed in other iron(III) trioxalates: 2.021 Å in $Li_4Fe(C_2O_4)_3Cl\cdot 9H_2O$,[1] 2.037 Å in $K_3Fe(C_2O_4)_3\cdot 3H_2O$[2] and 2.002 Å in $(NH_4)_3Fe(C_2O_4)_3\cdot 3H_2O$.[3] The distortion of the octahedron around the Fe^{3+} ion can be described quantitatively according to the formalism introduced by Muetterties and Guggenberger:[11] angle Φ describes the relative twist of opposed triangular faces of the octahedron, one face being composed of O(2), O(5), O(10) and the other of O(1), O(6), O(9). This way of choosing the opposite faces respects the approximate three-fold axis. The values of δ measure the angles between the normals to all the faces. In Table 3, the results obtained are compared with those observed in $Li_4Fe(C_2O_4)_3Cl\cdot 9H_2O$[1] and also with the values characterizing a regular octahedron and a trigonal prism. It appears that in both complexes, the coordination of the iron atom is an intermediate between these two regular polyhedra, with a marked preference for the octahedron. As previously pointed out by Declercq *et al.*,[1] the deformations of the octahedra can be related to the constraints imposed on the distance between the two oxygen atoms belonging to the same oxalate ion.

The coordinations of the three lithium ions are very different. $Li^+(1)$ shows a distorted octahedral

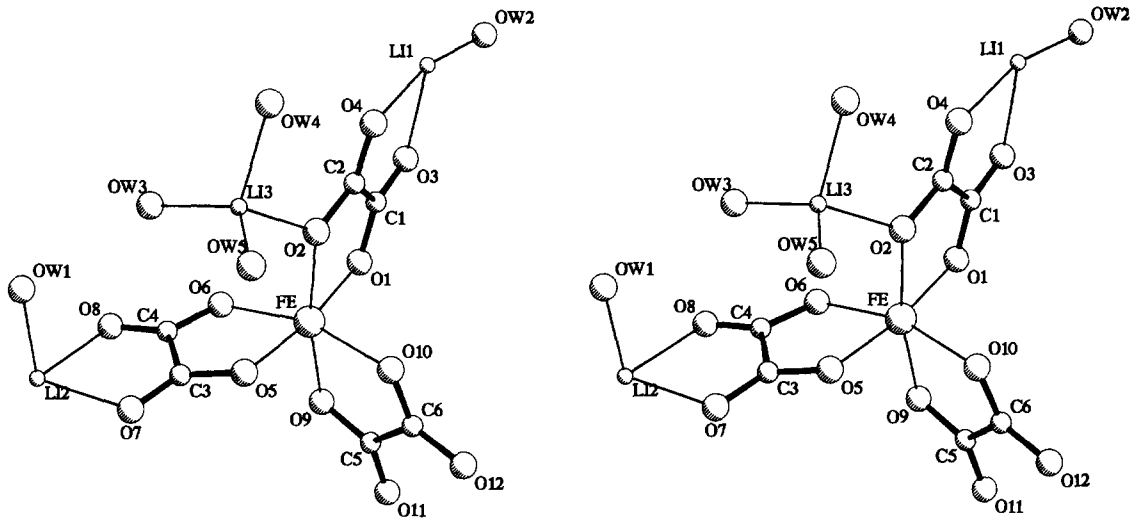

Fig. 2. Stereoscopic view showing the numbering of the atoms of the asymmetric unit and the octahedral coordination of the iron atom. Programme PLUTO.[10]

Table 2. Bond distances (Å) and angles (°)

The oxalate ion			
C(2)—C(1)	1.539(1)	C(2)—C(1)—O(1)	115.4(1)
C(1)—O(1)	1.271(1)	O(3)—C(1)—O(1)	126.3(1)
C(1)—O(3)	1.232(1)	C(2)—C(1)—O(3)	118.2(1)
C(2)—O(2)	1.284(1)	O(4)—C(2)—O(2)	126.6(1)
C(2)—O(4)	1.232(1)	C(1)—C(2)—O(2)	114.6(1)
		C(1)—C(2)—O(4)	118.8(1)
C(4)—C(3)	1.541(1)	O(7)—C(3)—O(5)	126.2(1)
C(3)—O(5)	1.280(1)	C(4)—C(3)—O(5)	114.9(1)
C(3)—O(7)	1.225(1)	C(4)—C(3)—O(7)	118.9(1)
C(4)—O(6)	1.288(1)	O(8)—C(4)—O(6)	126.9(1)
C(4)—O(8)	1.221(1)	C(3)—C(4)—O(6)	114.0(1)
		C(3)—C(4)—O(8)	119.1(1)
C(6)—C(5)	1.540(1)	O(11)—C(5)—O(9)	126.8(1)
C(5)—O(9)	1.279(1)	C(6)—C(5)—O(9)	115.0(1)
C(6)—O(10)	1.286(1)	C(6)—C(5)—O(11)	118.3(1)
C(5)—O(11)	1.229(1)	O(12)—C(6)—O(10)	126.8(1)
C(6)—O(12)	1.225(1)	C(5)—C(6)—O(10)	114.5(1)
		C(5)—C(6)—O(12)	118.7(1)
Octahedral coordination of Fe^{3+}			
O(1)—Fe	1.994(1)	O(2)—Fe—O(1)	81.16(4)
O(2)—Fe	2.035(1)	O(5)—Fe—O(1)	170.54(4)
O(5)—Fe	2.024(1)	O(5)—Fe—O(2)	92.53(4)
O(6)—Fe	2.009(1)	O(6)—Fe—O(1)	93.58(4)
O(9)—Fe	2.021(1)	O(6)—Fe—O(2)	100.23(4)
O(10)—Fe	2.005(1)	O(6)—Fe—O(5)	80.54(4)
		O(9)—Fe—O(1)	90.82(4)
		O(9)—Fe—O(2)	168.79(4)
		O(9)—Fe—O(5)	96.35(4)
		O(9)—Fe—O(6)	88.00(4)
		O(10)—Fe—O(1)	100.30(4)
		O(10)—Fe—O(2)	92.77(4)
		O(10)—Fe—O(5)	86.97(4)
		O(10)—Fe—O(6)	162.30(4)
		O(10)—Fe—O(9)	80.92(4)

Table 2.—*continued*

Octahedral coordination of $Li^+(1)$			
Li(1)—O(3)	2.072(3)	O(4)—Li(1)—O(3)	78.3(1)
Li(1)—O(4)	2.225(3)	$O(11)^v$—Li(1)—O(3)	90.2(1)
Li(1)—$O(4)^{iii}$	2.311(3)	$O(11)^v$—Li(1)—O(4)	98.4(1)
Li(1)—$O(11)^v$	2.082(3)	$O(12)^v$—Li(1)—O(3)	160.6(1)
Li(1)—$O(12)^v$	2.159(3)	$O(12)^v$—Li(1)—O(4)	86.9(1)
Li(1)—Ow(2)	2.078(3)	$O(12)^v$—Li(1)—$O(11)^v$	79.4(1)
		Ow(2)—Li(1)—O(3)	91.6(1)
		Ow(2)—Li(1)—O(4)	166.9(1)
		Ow(2)—Li(1)—$O(11)^v$	90.0(1)
		Ow(2)—Li(1)—$O(12)^v$	104.6(1)
		O(3)—Li(1)—$O(4)^{iii}$	109.4(1)
		Ow(2)—Li(1)—$O(4)^{iii}$	84.8(1)
		$O(11)^v$—Li(1)—$O(4)^{iii}$	159.7(1)
		$O(12)^v$—Li(1)—$O(4)^{iii}$	83.0(1)
		O(4)—Li(1)—$O(4)^{iii}$	90.5(1)
Octahedral coordination of $Li^+(2)$			
Li(2)—$O(3)^{ii}$	2.678(3)	$O(11)^i$—Li(2)—Ow(1)	153.7(2)
Li(2)—O(7)	2.075(3)	$O(11)^i$—Li(2)—O(7)	111.9(1)
Li(2)—$O(7)^{iv}$	2.073(3)	$O(11)^i$—Li(2)—$O(7)^{iv}$	93.1(1)
Li(2)—O(8)	2.186(3)	$O(11)^i$—Li(2)—O(8)	88.7(1)
Li(2)—$O(11)^i$	1.985(3)	$O(11)^i$—Li(2)—$O(3)^{ii}$	76.7(1)
Li(2)—Ow(1)	2.066(3)	Ow(1)—Li(2)—O(7)	94.3(1)
		Ow(1)—Li(2)—$O(7)^{iv}$	92.0(1)
		Ow(1)—Li(2)—O(8)	94.6(1)
		Ow(1)—Li(2)—$O(3)^{ii}$	77.8(1)
		$O(7)^{iv}$—Li(2)—O(7)	82.3(1)
		$O(7)^{iv}$—Li(2)—O(8)	161.1(1)
		$O(7)^{iv}$—Li(2)—$O(3)^{ii}$	115.5(1)
		O(7)—Li(2)—O(8)	79.6(1)
		O(7)—Li(2)—$O(3)^{ii}$	160.4(1)
		O(8)—Li(2)—$O(3)^{ii}$	83.2(1)
Tetrahedral coordination of Li^+ (3)			
Li(3)—O(2)	2.083(3)	Ow(3)—Li(3)—O(2)	105.0(1)
Li(3)—Ow(3)	1.942(3)	Ow(4)—Li(3)—O(2)	101.5(1)
Li(3)—Ow(4)	1.959(4)	Ow(4)—Li(3)—Ow(3)	111.7(2)
Li(3)—Ow(5)	1.927(4)	Ow(5)—Li(3)—O(2)	112.2(2)
		Ow(5)—Li(3)—Ow(3)	122.9(2)
		Ow(5)—Li(3)—Ow(4)	101.6(2)

(i) $-x, -y, -z$; (ii) $-x, -y+1, -z$; (iii) $-x+1, -y+2, -z+1$; (iv) $-x-1, -y, -z$; (v) $x, y+1, z$.

Table 3. Comparison of the deformations of the octahedra around Fe^{3+} ions in $Li_3Fe(C_2O_4)_3 \cdot 5H_2O$ (this study) and $Li_4Fe(C_2O_4)_3Cl \cdot 9H_2O$[1] using the symbolism proposed by Muetterites and Guggenberger;[11] the extreme situations, regular octahedron (O_h) and trigonal prism (D_{3h}), are indicated

	Φ	δ(b1)	δ(b2)	δ(remaining)
O_h (regular octahedron)	60.0	70.5	70.5	70.5
$Li_3Fe(C_2O_4)_3 \cdot 5H_2O$	44.5	55.5, 56.9, 59.4	81.0, 81.7, 85.9	68.9, 70.8, 71.0 72.4, 72.7, 73.2
$Li_4Fe(C_2O_4)_3Cl \cdot 9H_2O$[1]	46.0	59.3	82.2	70.5, 71.0
D_{3h} (trigonal prism)	0	0	120.0	90.0

surrounding composed of the two oxygen atoms (not bound to Fe^{3+}) of two oxalate ions acting as bidentate ligands, a water molecule and one oxygen atom [O(4)] of an oxalate ion, symmetry related to one of the previous ones. As shown in Table 2, the distance to this sixth ligand is appreciably longer (2.311 Å) than the others (mean value = 2.12 Å). A more or less similar situation occurs around $Li^+(2)$, but with one very long distance [2.678 Å for $Li^+(2)$—O(3)] completing the coordination. The mean value of the five other distances is 2.08 Å. In the coordination of $Li^+(2)$, only one oxalate acts as a bidentate ligand, and one water molecule is present. In both cases, i.e. the surroundings of $Li^+(1)$ and $Li^+(2)$, two neighbouring octahedra related by an inversion centre share one common edge, which is defined by two symmetry-related oxygen atoms: a line between O(4)···O(4) around $Li^+(1)$ and a line between O(7)···O(7) around $Li^+(2)$ (Fig. 3). As concerns $Li^+(3)$, the coordination is tetrahedral, composed of the three remaining water molecules and only one oxygen atom [O(2)] belonging to an oxalate ion (Fig. 2). It is worth noting that this oxygen atom also binds the Fe^{3+} ion and that it is the only oxygen atom shared between the iron ion and a lithium ion.

If one considers that the strongest bonds between a cation (Fe^{3+} or Li^+) and an oxalate anion are the bidentate arrangements involving two oxygen atoms of the same oxalate anion, an infinite chain appears, coincident with the direction of the crystallographic *b*-axis: $Li^+(1)$ and Fe^{3+} alternate between the oxalate anions, and two successive identical atoms along this chain are related by a translation of one unit cell (Fig. 4). If one compares this figure to Fig. 1 of the paper describing $Li_4Fe(C_2O_4)_3Cl \cdot 9H_2O$,[1] a striking similarity appears. In the latter case a kind of two-dimensional hexagonal tiling adequately described the structure. The apices of the hexagons were alternatively occupied by iron and lithium ions, and a hexahydrated chloride ion lies in the centre of the hexagon. In the present situation, only five apices exist (two iron and three lithium ions), the result being a one-dimensional chain instead of a two-dimensional sheet. Another important difference is that a trihydrated lithium ion [$Li^+(3)$] lies inside the "unclosed hexagons". As shown in Fig. 5, these one-dimensional chains are assembled together to produce a three-dimensional network by means of the remaining bonds (not bidentate) between the oxygen atoms of the oxalate ions and the lithium ions $Li^+(1)$ and $Li^+(2)$. The cohesion of the structure is reinforced by the formation of hydrogen bonds between the water molecules and oxygen atoms belonging to the oxalate ions or to other water molecules. The details of these hydrogen bonds are given in Table 4.

Mössbauer spectroscopy

The Mössbauer spectrum at 298 K of polycrystalline $Li_3Fe(C_2O_4)_3 \cdot 5H_2O$ is shown in Fig. 6a–c as a function of the fitting procedure. It consists of an asymmetric and strongly broadened absorption pattern, indicating the presence of paramagnetic relaxation effects.[13]

Attempts to fit the spectrum with a single Lorentzian line gave the wrong χ^2 value (2.3316) and an isomer shift (I.S. = 0.27 ± 0.05 mm s^{-1}) which is somewhat smaller than one would expect for a high spin Fe^{3+} ion (Fig. 6a).

Assuming the presence of a small quadrupolar interaction as being responsible for the spectrum asymmetry, a two-Lorentzian-line fit results in a better χ^2 value (0.9732; Fig. 6b) and in apparent quadrupole splitting (Q.S. = 0.31 ± 0.05 mm s^{-1}) and isomer shift values (I.S. = 0.32 ± 0.05 mm s^{-1}) which are consistent with a high spin Fe^{3+} ion in a non-cubic environment. This assumption is indeed well supported by the above described deformation of the octahedral coordination of the iron atom from O_h to D_{3h} symmetry. However, in this fitting procedure, both intensities and widths of the two lines were not constrained to be equal; as a result, the intensity ratio I^+/I^- of the highest energy line (I^+) to the lowest one (I^-) is found to be equal to 2.94, whereas the line width of the I^+ line is larger (3.21 ± 0.07 mm s^{-1}) than that of the I^- one (0.91 ± 0.07 mm s^{-1}). As already mentioned,[1] in the case of $Li_4Fe(C_2O_4)_3Cl \cdot 9H_2O$, the asymmetry of the line widths can be attributed to relaxation of paramagnetic ions causing fluctuating magnetic fields. If the fluctuating magnetic field is parallel to the electric field gradient, Blume and Tjon[14] have shown that the $|\pm 3/2\rangle$ to $|\pm 1/2\rangle$ nuclear transitions which make up one of the lines (I^+) of the quadrupole doublet have a larger splitting than do the $|\pm 1/2\rangle$ to $|\pm 1/2\rangle$ transitions, which make up the other line (I^-). For the complex $Li_3Fe(C_2O_4)_3 \cdot 5H_2O$, the observed line widths are much broader than those of the previously described compound $Li_4Fe(C_2O_4)_3Cl \cdot 9H_2O$ ($I^+ = 1.58$ mm s^{-1}; $I^- = 0.80$ mm s^{-1}); this result indicates a slower relaxation process in the former compound, for which the distance between the nearest Fe^{3+} ions is found to be larger (Fe—Fe = 6.559 Å) than the one found[1] in the latter complex (Fe—Fe = 5.356 Å).

In the case of a randomly distributed polycrystalline sample and in the absence of the Goldanskii–Karyagin effect, the intensity ratio I^+/I^-

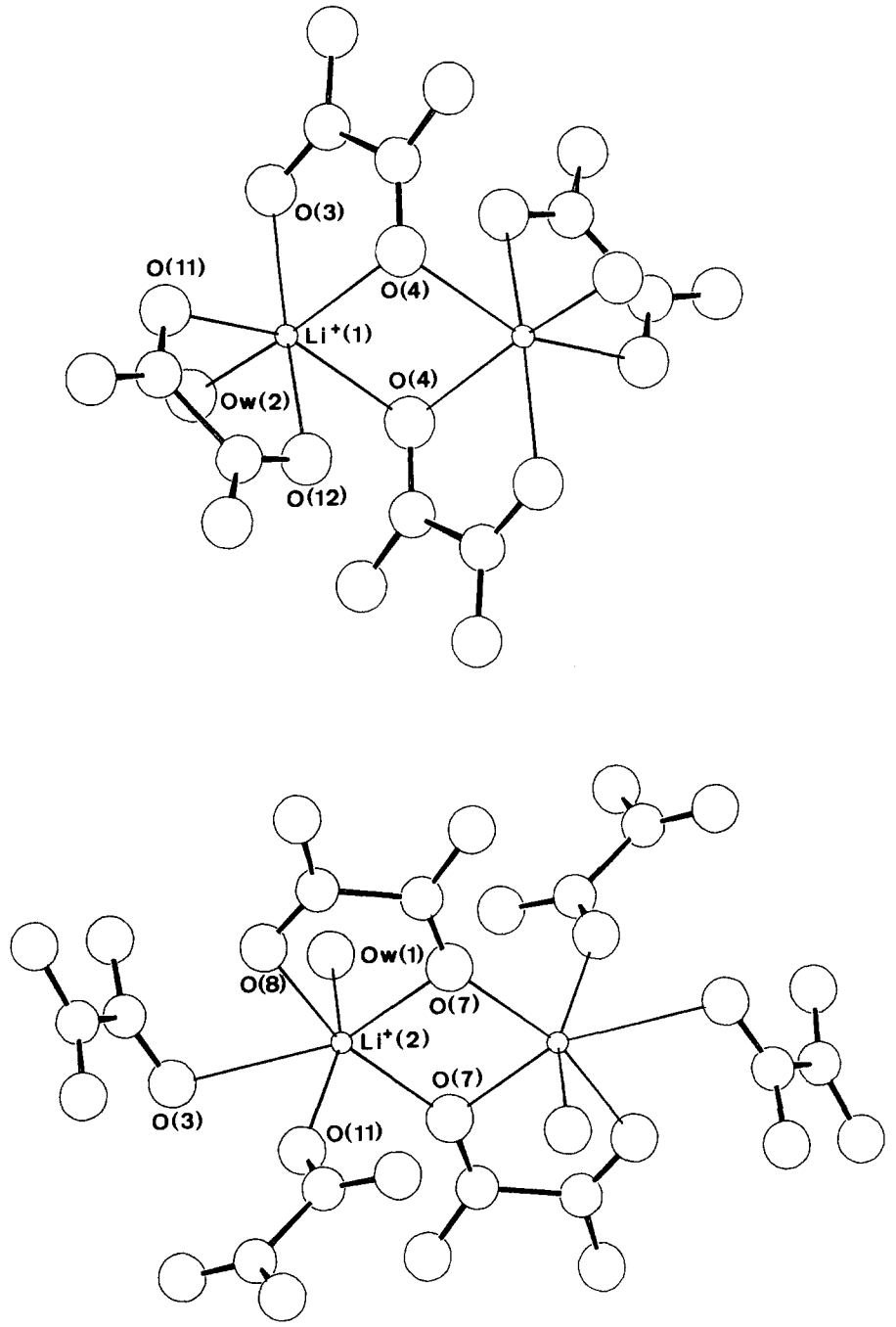

Fig. 3. The coordination of $Li^+(1)$ and $Li^+(2)$. In both cases, two neighbouring octahedra related by an inversion centre share one common edge, respectively, defined by the line O(4) ··· O(4) and the line O(7) ··· O(7). Programme ORTEP.[12]

should be equal to unity. It is likely that the larger value observed here has to be attributed to the approximate fitting procedure used, which does not take into account all the spectral components in the case of relaxation broadening. It has been shown[15] that the central part of the I^- line is accompanied by a very broad line of small amplitude, the area of which can be up to 20–30% of the total area. A better interpretation of the spectrum line shape can be achieved by using a sum of three Lorentzians whose intensities and widths can be analytically given for special hypothesis concerning spin–spin relaxation process.[16] This procedure yields, with a good χ^2 value (0.9900), a better value of the I^+/I^- ratio (1.41 ± 0.40), but gives rise to larger values for both quadrupole splitting (Q.S. = 0.47 ± 0.05 mm

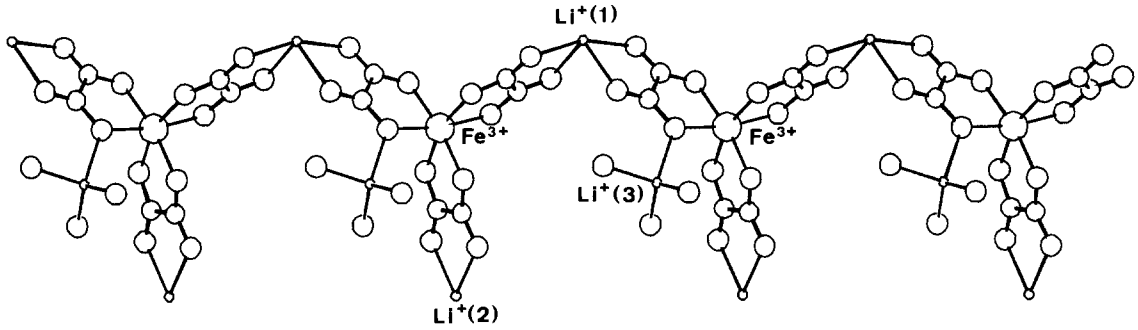

Fig. 4. Infinite chain coincident with the direction of the crystallographic *b*-axis: $Li^+(1)$ and Fe^{3+} alternate between the oxalate anions. Programme ORTEP.[12]

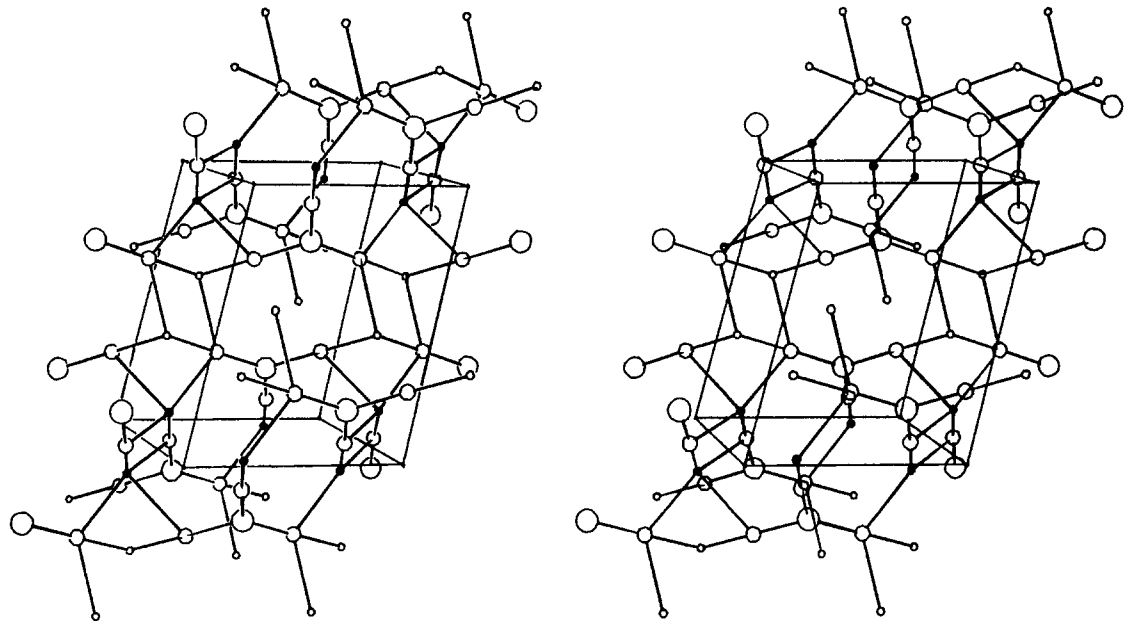

Fig. 5. Stereoscopic view of the three-dimensional network created by the bonds between the oxalate anions and the cations [Fe^{3+}, $Li^+(1)$ and $Li^+(2)$]. To avoid overcrowding, the oxalate anions are represented as simple spheres. (○) $Li^+(1)$, (•) $Li^+(2)$, (o) oxalates, (O) Fe^{3+}. The view is approximately parallel to the *b*,*c*-plane, with the *b*-axis horizontal. Programme ORTEP.[12]

Table 4. Hydrogen bonds involving the water molecules

Donor	Acceptor	Distance (Å)	Symmetry operation applied to the acceptor
Ow(1)	O(9)	2.819	$x-1, y, z$
	Ow(3)	3.137	$-x-1, -y+1, -z$
Ow(2)	O(5)	2.810	$x+1, y+1, z$
	Ow(4)	2.964	$-x+1, -y+2, -z+1$
Ow(3)	Ow(1)	2.848	
	O(6)	2.801	$-x, -y+1, -z$
Ow(4)	O(3)	2.804	$x-1, y, z$
	O(4)	2.836	
Ow(5)	Ow(2)	2.846	$x-1, y-1, z$
	O(10)	2.865	$-x, -y+1, -z+1$

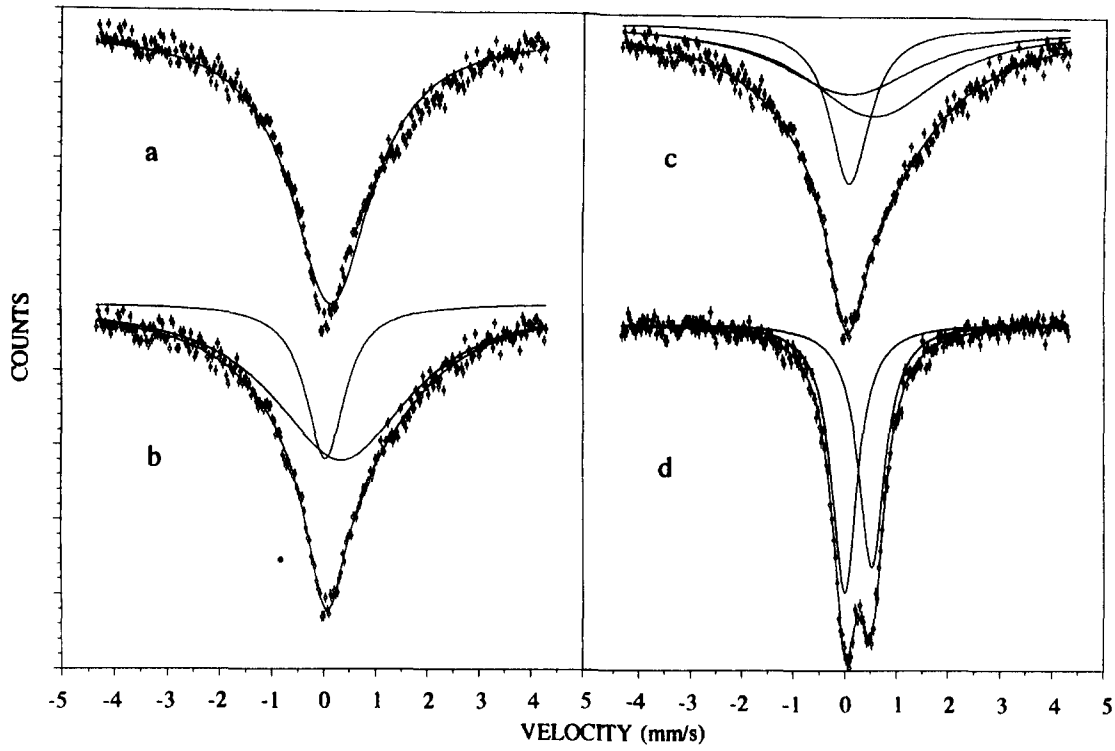

Fig. 6. Mössbauer spectra at 298 K of $Li_3Fe(C_2O_4)_3 \cdot 5H_2O$ (a–c) as a function of the fitting procedure (see text) and of $Li_3Fe(C_2O_4)_3$ (d).

s^{-1}) and isomer shift (I.S. $= 0.38 \pm 0.05$ mm s^{-1}) (Fig. 6c). A similar computer fit has already been applied by Barb *et al.*[17] to alkali trisoxalatoferrate(III) complexes for which, unfortunately, no information was given on the hydration number of the compounds nor on the quadrupole splitting and isomer shift values. Nevertheless, an electronic relaxation time of 4.3×10^{-9} s was found in the case of the lithium complex, assuming an isotropic relaxation model. This value is characteristic of an intermediate relaxation time, which is of the order of the radiative lifetime of the excited nuclear level, i.e. about 10^{-8} s.

The influence of the relaxation time on the shape of the quadrupole doublet is well illustrated in the case of anhydrous lithium trisoxalatoferrate(III), $Li_3Fe(C_2O_4)_3$, a compound which can be prepared, according to thermogravimetric analysis (Fig. 1), by dehydration of a pentahydrate at 200°C. Although the Mössbauer spectrum of $Li_3Fe(C_2O_4)_3 \cdot 5H_2O$ consists of a broad and asymmetric peak due to an intermediate relaxation process, the spectrum of the anhydrous compound (Fig. 6d) exhibits a well resolved but slightly asymmetric quadrupole doublet (Q.S. $= 0.52 \pm 0.05$ mm s^{-1}; I.S. $= 0.37 \pm 0.05$ mm s^{-1}) with much narrower line widths (I^+ : 49%, 0.62 mm s^{-1}; I^- : 51%, 0.60 mm s^{-1}). The difference between the Mössbauer spectra of the pentahydrated and anhydrous lithium trisoxalatoferrate(III) implies that the spin–spin relaxation time decreases in the anhydrous compound compared with the hydrous compound because of the decreased average Fe—Fe distance.

It is also noteworthy that the isomer shift of the anhydrous complex is very close to the value found for the pentahydrate by using a three-Lorentzian analysis, which confirms the reliability of this fitting procedure. In addition, the quadrupole splittings of both compounds are comparatively of the same order of magnitude, presumably because the deformations of the iron octahedral coordination are very similar, being mostly induced by the constraints imposed by the oxalate groups in the bonding of $[Fe(C_2O_4)_3]^{3-}$. It would therefore be highly interesting to proceed to a crystal structure analysis of the anhydrous complex, and experiments are now in progress to produce single crystals of this material.

REFERENCES

1. J. P. Declercq, J. Feneau-Dupont and J. Ladrière, *Polyhedron* 1993, **9**, 1031.
2. P. Herpin, *Bull. Soc. Fr. Min. Crist.* 1958, **146**, 185.

3. E. H. Merrachi, B. F. Mentzen, F. Chassagneux and J. Bouix, *Rev. Chim. Min.* 1987, **9**, 56.
4. J. Ladrière and D. Apers, *Hyperfine Int.* 1988, **42**, 1055.
5. J. Ladrière, *Hyperfine Int.* 1992, **70**, 1095.
6. J. Ladrière, *Hyperfine Int.* 1992, **70**, 1091.
7. J. Akashi, Y. Uchida, T. Komjina, M. Katada and H. Sano, *Bull. Chem. Soc. Japan* 1984, **57**, 1076.
8. G. M. Sheldrick, SHELXS86, in *Crystallographic Computing* 3 (Edited by G. M. Sheldrick, C. Kruger and R. Goddard), pp. 175–189. Oxford University Press (1985).
9. G. M. Sheldrick, SHELX76. Program for Crystal Structure Determination. University of Cambridge, U.K. (1976).
10. W. D. S. Motherwell and W. Clegg, PLUTO, Program for Plotting Molecular and Crystal Structures. University of Cambridge, U.K. (1978).
11. E. L. Muetterties and L. J. Guggenberger, *J. Am. Chem. Soc.* 1974, **96**, 1748.
12. C. K. Johnson, ORTEP. A Fortran Thermal-ellipsoid Plot Program for Crystal Structure Illustrations. Oak Ridge National Laboratory, ORNL-3974 (1971).
13. D. Barb, L. Diamandescu and D. M. Tarabasan, *J. Phys.* 1976, **C6-37**, 113.
14. M. Blume and T. A. Tjon, *Phys. Rev.* 1968, **165**, 446.
15. N. Trane and G. Trumpy, *Phys. Rev.* 1970, **1**, 153.
16. A. M. Afans'ev and V. D. Gorobchenko, *Zh. Eksp. Teor. Fiz.* 1974, **66**, 1406.
17. D. Barb, L. Diamandescu and D. M. Tarabasan, *J. Phys.* 1980, **C1-1**, 227.